Nitrogen-modified nanoporous activated carbon from eucalyptus leaves for ultrasound-assisted removal of basic dyes using derivative spectrophotometric method

AISAN KHALIGH[1]*, HASSAN ZAVVAR MOUSAVI[1], ALIMORAD RASHIDI[2]
and HAMID SHIRKHANLOO[3]

[1]*Department of Chemistry, Semnan University, Semnan 35131-1911, Iran, [2]Nanotechnology Research Center, Research Institute of Petroleum Industry (RIPI), West Entrance Blvd., Olympic Village, Tehran 14857-33111, Iran and [3]Research Institute of Petroleum Industry (RIPI), West Entrance Blvd., Olympic Village, Tehran 14857-33111, Iran*

Abstract: The nanoporous activated carbon (AC) was prepared from the eucalyptus leaves *via* chemical activation with KOH, then treated with nitric acid/ /urea (NOAC) and finally used as a new adsorbent for simultaneous ultrasound-assisted removal of basic red 46 (BR46) and basic yellow 13 (BY13) dyes from binary aqueous solutions. The NOAC nano-adsorbent was characterized with SEM, TEM, Raman, BET, FTIR, CHN, pH_{pzc} and Boehm titration analysis. Both of the AC and NOAC samples had superior BET surface area of 2222 and 1572 m^2 g^{-1} with average micropore volume of 0.81 and 0.50 cm^3 g^{-1}, respectively. First order derivative spectrophotometric method was used for analysis of BY13 in binary mixtures. Small amount of the adsorbent (30 mg) was capable to remove high percentage of dyes (>99 %) in a very short time (8 min). The adsorption of dyes follows the Langmuir isotherm and the pseudo--second-order kinetics. The adsorption capacities of NOAC for single solutions of BR46 and BY13 were 1111 and 1250 mg g^{-1} as well as for binary solutions were 769 and 909 mg g^{-1}, respectively. The adsorption thermodynamics were also explored. Exhausted NOAC was regenerated using HCl (2 M) and reused for five adsorption-desorption cycles with high performance.

Keywords: low-cost adsorbent; cationic dyes; fast adsorption; isotherm; kinetics; thermodynamics.

INTRODUCTION

Industry dyes are becoming worldwide sources of environmental pollution, and their existence has severely affected the aquatic organisms and life cycle. One of the most problematic classes of dyes are the basic dyes called cationic

dyes.[1] Toxic cationic dyes of basic red 46 (BR46, single azo class) and basic yellow 13 (BY13, azomethine class) are widely used in acrylic, nylon, silk, leather and wool dyeing process. These dyes have carcinogenic, mutagenic, and teratogenic properties which may be related to the presence of nitrogen and positive charge on their structures.[2]

Dyes are particularly difficult to remove by conventional waste treatment methods since they are recalcitrant organic molecules, resistant to aerobic digestion and are stable to light, heat and oxidizing agents. Herein, the removal of dyes from water in an economical way remains an important challenge to scientists. Processes such as coagulation/flocculation, membrane filtration, ion exchange and adsorption are also used for treating dye containing wastewater.[3] The later method gain major superiority due to its proven efficiency, the ease of use and the insensitivity to toxic material without resulting in the formation of harmful substances as well as the availability of a wide range of adsorbents.[4]

Adsorption by the activated carbon has been widely used for wastewater treatment due to its exceptionally high surface area and micropore volume, well--developed internal microporosity, favourable pore size distribution, and high adsorption efficiency together with the availability of low-cost resources such as plant residues. Recently, an enormous range of waste agricultural materials have been used as activated carbon precursors including rice husk, fruit stone, palm shell, almond shell, coconut shell, pistachio-nut shell, sugar cane bagasse, spent tea leaves, and reedy grass, *etc*.[5] In general, raw materials are initially treated to form charcoal. Then, physical or chemical activation of the charcoal results in activated carbons.[6]

Recently, much attention has been paid to the surface modification of the activated carbons,[7] The conventional protocols used for the modification are oxidation, nitrogenation, sulfuration and coordinated ligand anchora.[7] The introduction of nitrogen functional groups onto the surface of AC and replacing them with the existing oxygen groups has become a subject of great interest nowadays.[7,8] In this trend, oxidation pretreatment of the AC can enhance the incurporation of nitrogen into the carbon.[9] Nitrogen modification of AC is an effective method which increases its basicity, polarity of its surface and hence the specific interaction with polar adsorbates. In order to incorporate of nitrogen into the carbon structure, carbons are treated with ammonia, urea, dicyanodiamine, *N,N*--dimethylformamide, melamine or their derivatives, in the temperature range from 350 to 900 °C, in different periods of time under nitrogen.[9,10] It has been reported that the basic nitrogen functional groups such as amine groups ($-NH_2$, $-NH$) can be introduced by the urea treatment of AC at low temperatures range, from 350 to 500 °C.[10] The presence of the heterocyclic nitrogen compounds incorporated in the carbon matrix with free pairs of electrons increase the electron donor capacity of the solid. Therefore, the nitrogen-containing ACs are the

effective adsorbents of positively charged pollutants such as heavy metal ions and cationic dyes through the formation of donor–acceptor complexes.[9] Nitrogen-modified ACs have successfully been applied in the water decontamination treatments for the removal of heavy metal ions (Cu(II), Pb(II), Hg(II) and Cd(II)),[7,11,12] anions (CN^-, ClO_4^-, AsO_4^{3-}),[7,11] organic substances (benzoic acid, phenol, atrazine),[7,13] and natural organic matter. Herein, their adsorption was generally enhanced on nitrogenated ACs versus virgin ACs.

The UV–Vis spectrophotometric method is usually used as a simple, economic, rapid and accurate technique for dye assessments.[14] However, the simultaneous analysis of dyes in binary solution by the spectrophotometric methods can be very complex due to the overlapping absorption bands of the dyes and spectral interferences. Derivative spectrophotometry is an analytical technique of great utility for overcomming this limitation. The derivatization of the zero order spectrum can lead to the separation of overlapped signals and to the elimination of background caused by the presence of the other compounds in a sample.[2,15]

In this study, a low-cost nanoporous activated carbon with a large surface area was prepared from eucalyptus leaves through KOH activation, then treated with nitric acid and urea (NOAC) and finally used as a new nanoadsorbent for the simultaneous ultrasound-assisted removal of basic red 46 (BR46) and basic yellow 13 (BY13) dyes from binary solutions. Eucalyptus leaves, as a raw material for the production of activated carbon, can be considered as one of the best candidates among the agricultural wastes because it is cheap and quite abundant, especially in arid and semiarid areas like Semnan, Iran. The first derivative spectrophotometric method was used for analysis of BY13 in binary mixtures. The influence of several parameters such as pH, temperature, initial concentration of dyes, adsorbent dosage and ultrasonication time for the maximum removal of both dyes was investigated, using the batch adsorption method. Furthermore, the characterization of dye adsorption was described by the kinetics models, adsorption isotherms and thermodynamic parameters.

EXPERIMENTAL

Apparatus and characterization methods

A double beam UV–Vis spectrophotometer (Shimadzu, model PC 1650-UV, Japan) with two matched 1-cm quartz cells was used for the analysis of the studied dyes. The pH measurements were carried out using a digital pH meter (Metrohm, model 744, Herisau, Switzerland). The ultrasonic bath with heating system (Tecno-GAZ SPA Ultra Sonic System) and a centrifuge (Hettich, model EBA 20, Germany) were used in the batch adsorption experiments.

The surface morphology of the adsorbent was characterized using a scanning electron microscopy (SEM, Phillips, PW3710, Netherland) and a transmission electron microscopy (TEM, CM30, Philips, the Netherlands). The textural parameters of the prepared samples including surface area, pore volume, and pore size distribution were determined by the nitrogen adsorption–desorption isotherms at 70 K using a Micrometrics ASAP 2010 system (Micrometric Instruments Co, Cleveland, OH, USA). The specific surface area was calculated by

the BET (Brunauer–Emmett–Teller) method. The total pore volume was obtained from the volume of nitrogen adsorbed at the relative pressure of 0.99. The micropore analysis was performed by the t-plot method (a technique which allows determining the microporous volumes and the specific surface area of a sample by comparison with a reference adsorption isotherm of a nonporous material having the same surface chemistry) and mesopore volume was determined from desorption branch of the isotherm by the BJH (Barrett, Joyner and Halenda) method. The pore size distribution was determined as well. The average pore diameter was also given by $4V_{total}/S_{BET}$. Prior to the analysis the samples were degassed under vacuum at 200 °C for 2 h. Raman spectroscopy was carried out with an Almega Thermo Nicolet and 532 nm Ar-ion laser excitation source in order to investigate the structural properties and bonding in the virgin and modified ACs. The elemental composition of the samples was measured using the CHN elemental analyzer (Euro Vector S.P.A, model EA 3000, Italy). The oxygen content was calculated as a difference between 100 % and the sum of C+H+N. The Fourier transform infrared (FT-IR) spectra were recorded in the range from 4000 to 400 cm^{-1} using a Bruker IFS 88 spectrometer (Bruker Optik GmbH, Ettlingen, Germany) with KBr pelleting method. The surface acidic and basic groups of the prepared samples were estimated using Boehm titration method. 0.5 g of the activated carbon samples were added in test tubes containing 25 mL of NaOH, Na_2CO_3, $NaHCO_3$, or HCl (0.05 M). The test tubes were shaken for 24 h at 25 °C and filtrated. Then, 5 mL of the filtrate was pipetted and the excess of base or acid was titrated with HCl or NaOH (0.1 M) solution. The Metrohm pH-meter was employed to monitor the titration. The numbers of acidic sites and basic sites were calculated using the titration result.[16] The pH_{PZC} (point of zero charge) of the sorbents was determined using the known method as was detailed before.[17]

Chemical reagents and solutions

All chemicals, with analytical grade purity available, were purchased from Merck (Darmstadt, Germany). Basic Red 46 (BR46) and Basic Yellow 13 (BY13), as model dyes, were used without further purification. The chemical structure and properties of the dyes are shown in Table S-I of Supplementary material to this paper. Deionised water (DI-water) from a Millipore Continental Water System (Bedford, MA, USA) was used for the preparation of the aqueous solutions. The stock solution of each dye (1000 mg L^{-1}) was prepared by dissolving 250 mg of the dye in 250 mL of DI-water. The experimental and working standard solutions were prepared daily by the dilution of the stock solutions.

Preparation of nanoporous activated carbon

The eucalyptus leaves (EL) as a raw material for the preparation of AC were obtained from Semnan city, north central Iran. The collected EL was washed with distilled water to remove all the dirt particles, then dried at room temperature for 24 h, and finally ground to powder in a laboratory blender to attain particle size of 0.4–0.8 mm. The EL-based activated carbon was prepared via two steps; carbonization of the dried precursor under an inert atmosphere followed by the chemical activation of the char impregnated with potassium hydroxide. KOH was used as the chemical activating agent as it is one of the most effective compounds for the production of activated carbons. Details are as follows: the resulting EL powder was first carbonized at 600 °C for 1 h under N_2 flow (200 mL min^{-1}) in a stainless steel tube furnace (1500 mm×50 mm) at a heating rate of 5 °C min^{-1} up to 600 °C. The prepared EL-char was then cooled to room temperature under N_2 flow and removed from the reactor.

Nanoporous activated carbon was prepared by mixing the EL-char with KOH solution (KOH:char weight ratio of 2.5:1) at room temperature for 1 h. The slurry was dried overnight

at 120 °C. Then, the impregnated sample was pyrolyzed in the stainless steel tube furnace under N_2 flow (200 mL min^{-1}) at the activation temperature of 850 °C, the holding time of 1 h and the heating rate of 5 °C min^{-1}. After the activation process, the obtained AC was cooled down to room temperature under N_2 flow. Then, in order to obtain the pure AC and remove any residual organic and mineral matter, the product was mixed with HCl solution (50 vol.%) for 2 h and then washed with hot and cold deionised water until pH of 6–7 was attained. Finally, EL-based nanoporous AC was oven dried at 100 °C.

Nitrogen modification of nanoporous activated carbon

The AC surface was first treated with HNO_3 solution. 3 g of nanoporous AC was immersed in a flask containing 100 mL of aqueous HNO_3 solution (50 vol.%) and stirred under reflux at 60 °C for 3 h. The oxidized AC (OAC) was then cooled to room temperature, washed repeatedly with DI-water until the filtrate was neutral and finally dried overnight at 70 °C.

In order to prepare the nitrogen-modified nonporous AC (NOAC), urea was used as a nitrogen-rich precursor. 1 g of OAC was impregnated with 10 ml of urea solution (1 M) at room temperature for 2 h. The mixture was oven dried at 80 °C. Then, the dried sample was annealed by using stainless steel tube furnace at 450 °C for 1 h in the N_2 atmosphere (200 mL min^{-1}) at a heating rate of 5 °C min^{-1} up to 450 °C. The obtained product was cooled down to room temperature under N_2 flow, washed with boiling DI-water to remove the unreacted urea and finally oven dried at 60 °C for 6 h.

Ultrasound-assisted adsorption procedure

Ultrasound-assisted adsorption experiments were conducted using the batch method to elucidate the effect of various parameters such as the solution pH, the ultrasonication time, the adsorbent dose, the temperature and the initial dye concentration on the removal of dyes from binary solutions.

The necessary amount of NOAC was added to a 250 mL Erlenmeyer flask containing 100 mL of binary dye solution with the initial concentration of 150 mg L^{-1} (from each of BR46 and BY13) at desired pH value. The solution pH was adjusted by adding the negligible volumes of NaOH or HCl diluted solutions. The flask was immersed in an ultrasonic bath (40 kHz, 130 W) at 25 °C. An aliquot of the sample solution was withdrawn at the pre-determined time intervals and centrifuged at 3000g for 1 min. Finally the solution was analyzed for the final concentration of dyes by using the UV–Vis spectrophotometer. The removal percentage (R / %) and the solid phase dye concentration, q_e, mg g^{-1}, was calculated.

Adsorption isotherm

For single and binary dye solutions, the isotherm studies were carried out at different dye concentrations (Table S-II of the Supplementary material), pH 9 and 25 °C with 30 mg NOAC and 8 min ultrasonication time, according to the above adsorption procedure.

Adsorption kinetics

Kinetics of the dyes adsorption from binary solutions by NOAC were also investigated according to the adsorption procedure using different ultrasonication times (2–8 min) at the optimum values of pH, the adsorbent dosage and the temperature, obtained from the batch optimization procedure, *i.e.*, 9, 30 mg and 25 °C, respectively.

Adsorption thermodynamics

Thermodynamic studies at different temperatures (15–55 °C) were carried out by adding 20 mg of NOAC into 100 mL of binary dye solutions (150 mg L^{-1}). The solution pH and ultrasonication time were adjusted at 9 and 8 min, respectively.

Desorption studies

Initially, the batch adsorption tests were carried out on the fresh NOAC with 100 mL of 150 mg L^{-1} binary dyes solution at pH 9, containing 30 mg of NOAC. After mixing for 8 min with ultrasonic bath (40 kHz, 130 W, 25 °C), the mixtures were centrifuged (1 min, 3000g) and the residual concentrations of dyes in the supernatant solutions were similarly analyzed using UV–Vis spectrophotometer.

The spent NOAC separated from the solution was washed with DI-water to remove the unabsorbed dyes and then oven dried at 70 °C for 3 h. To choose the effective solvent for desorption of the retained dyes on NOAC, 30 mg of the loaded adsorbent was separately added into 100 mL of various acid-base solutions (HCl, NaOH, H$_2$SO$_4$, CH$_3$COOH) with different concentrations (1–3 mol L^{-1}). The resulting mixtures were agitated for the same time duration as the adsorption tests (*i.e.*, 8 min) in the ultrasonic bath (40 kHz, 130 W, 25 °C). After desorption, the concentrations of BY13 and BR46 desorbed, c_{de} (mg L^{-1}), were similarly determined using UV–Vis spectrophotometer. The desorption percentage was also calculated.

RESULTS AND DISCUSSION

Characterization of adsorbent

TEM image (Fig. 1a) of NOAC shows the porous structure of this sample with pore sizes less than 50 nm. Moreover, as can be seen in Fig. 1, the carbon layers shift to the graphene sheet as indicated by the arrow. This structure causes an increase in the surface area and the pore volume of the nanoadsorbent. The SEM image (Fig. 1b) also confirmed the porous morphology of the sorbent. The activation stage produced the extensive external surfaces with quite irregular cavities and pores.

The nitrogen adsorption isotherms for the pristine and the nitrogen-modified nanoporous AC samples are displayed in Fig. 1c. The corresponding isotherm curves of both samples exhibit isotherms of Type I, which is the characteristic of the microporous materials. The BJH pore size distribution curves (Fig. 1d) for both samples confirm the presence of the microporosity and also of small mesopores in the range of 2–5 nm. The textural properties of AC and NOAC are presented in Table I. The results show that the EL-based nanoporous AC have the extremely high BET surface area of 2222 m^2 g^{-1} and the significant micropore volume of 0.83 cm^3 g^{-1}. The obtained BET surface area is attributed to the decline of O$_2$, H$_2$ and N$_2$ contents of the precursor, during successive activation steps, creating a nanoporous carbon adsorbent with high porosity and surface area. After the modification, the surface area decreased to 1572 m^2 g^{-1} with the decrease of the micropore volume. This is due to the oxidation-nitrogenation reactions, which produced functional groups on the surface of AC.

Figs. 1e and f show the Raman spectra of AC and NOAC. As it can be seen in Fig. 2e, the virgin AC shows two broad peaks at about 1345 and 1594 cm^{-1}, assigned to D-band and G-band, respectively. For NOAC (Fig. 1f), D and G bands were slightly shifted up to 1350 and 1596 cm^{-1}, respectively, which may be related to the changes in the hydrogen content of AC sample. The I_D/I_G ratio

(the intensity ratio of the D and G bands) for AC and NOAC was found to be 1.46 and 1.43, respectively, which confirms the presence of the defective and the amorphous carbon structures in the both samples. Moreover, a shoulder which appears at around 1110–1140 cm^{-1} is attributed to the presence of some sp^2-hybridized structures in both samples.
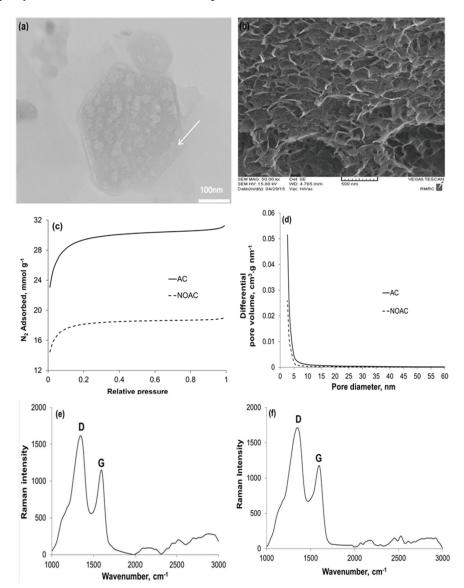

Fig. 1. a) TEM image of NOAC, b) SEM image of NOAC, c) nitrogen adsorption isotherms of AC and NOAC, d) BJH pore size distribution of AC and NOAC, e) Raman spectrum of AC, and f) Raman spectrum of NOAC.

TABLE I. Textural properties of pristine and nitrogen-modified AC

Sample	BET suface area $m^2\ g^{-1}$	Total pore volume $cm^3\ g^{-1}$	Micropore volume $cm^3\ g^{-1}$	Mesopore volume $cm^3\ g^{-1}$	Average pore diameter, $4V_{total}/S_{BET}$, nm	Average particle size, nm
AC	863	2.67	52.2	0.42	0.84	5.59
NOAC	626	2.62	42.2	0.27	0.41	5.59

C, H, N, O contents of the pristine and modified AC samples were presented in Table II. From the results, compared with the pristine AC, OAC had higher O content, originating from the oxidation reaction. Also, it is obvious that the urea treatment of the OAC led to an incorporation of a significant amount of nitrogen, instead of the surface oxygen groups and therefore NOAC has the low O content, compared to OAC.

TABLE II. Elemental analysis of pristine and modified AC samples (content, wt. %); O content = 100 – CHN content

Sample	Element			
	C	H	N	O
AC	85.07	2.74	0.62	11.57
OAC	74.22	1.78	0.85	23.15
NOAC	77.02	1.85	5.98	15.15

Oxidation and nitrogenation of AC were further confirmed using the Boehm titration method. As can be seen in Table III, the oxidation of AC increased total acidity, especially the value of carboxylic acid groups. Modification of OAC with urea resulted in the replacement of the surface oxygen groups with the nitrogen functional groups such as amine groups, so the basicity increased and the total acidity decreased. The FT-IR spectra of the modified AC samples were also recorded. Details about the FT-IR spectra are presented in Supplementary material (Fig. S-1a and b).

TABLE III. Content of functional groups of pristine and modified AC samples (mmol g^{-1}) determined by Boehm titration method
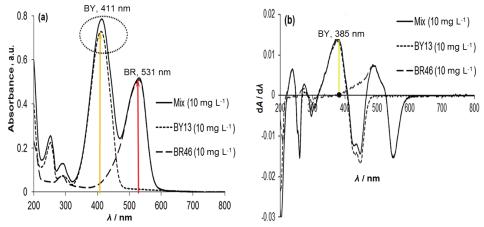
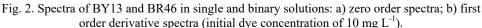| Sample	Group				
	Phenolic	Lactonic	Carboxylic	Total acidic	Basic
AC	0.210	0.096	0.184	0.480	0.425
OAC	0.510	0.643	1.024	2.177	0.231
NOAC	0.129	0.105	0.124	0.357	1.826

For the determination of pH_{PZC} of the synthesized samples, the final pH values were plotted versus their corresponding initial pH values (Fig. S-2 of the Supplementary material). The pH_{PZC} was taken as the point at which the curve crossed the line; pH_{final} equals to $pH_{initial}$. From the results, pH_{PZC} of AC, OAC

and NOAC were 6.3, 5.5 and 7.9, respectively. It is obvious that the pH_{PZC} of NOAC is higher than 7 (in the basic range), due to having the nitrogen functional groups that are naturally basic; while AC and OAC were acidic, due to the acidic oxygen functionalities.

The analysis of the single solutions and simultaneous analysis of the binary solutions

After preparation of the single solutions of BY13 and BR46 with the concentration of 10 mg L^{-1}, the zero order absorption spectra of these solutions were recorded between 200 and 800 nm (Fig. 2a). The maximum absorbance of BR46 and BY13 dyes in their single solutions were obtained at 530 and 411 nm, respectively. As shown in Fig. 2a, the absorption spectrum of BY13 dye in binary solution overlapped. Hence, it was not possible to estimate the amount of BY13 dye by the direct absorbance measurement in binary solutions. This problem was solved using the derivative spectrophotometric method. The first-order derivative spectrophotometry (Fig. 2b) showed that the wavelength of 385 nm should be used for the analysis of BY13 in the binary dye solution, where the absorbance of BR46 is zero. Therefore, the first and the zero order derivative spectrophotometric methods were utilized for the analysis of BY13 and BR46 in binary solutions at 385 ($^{1}D_{385}$) and 530 nm ($^{0}D_{530}$), respectively, and then calibration curves were made in the concentration range of 2–20 mg L^{-1} of the binary dyes solution (R^2 of 0.9995 and 0.9990 was found, respectively).

Fig. 2. Spectra of BY13 and BR46 in single and binary solutions: a) zero order spectra; b) first order derivative spectra (initial dye concentration of 10 mg L^{-1}).

In order to evaluate the accuracy of the zero and the first order derivative methods for determining of the BR46 and BY13 concentrations in binary solutions, the recovery studies were done. For this, the binary dye solutions with

different concentrations of both components were prepared; then the absorbance spectra of these solutions were taken and differentiated (Fig. S-3 of the Supplementary material). The calibration curve of each dye was made and the concentration of the BR46 and BY13 dyes was easily determined (see Table S-III of the Supplementary material). The recoveries, and the errors between the measured (c_m) and theoretical (c_t) concentrations were calculated.

From Table S-III, the high and reasonable recoveries (95–103 %) and the low error values (<5 %) show the efficiency of this method for the accurate analysis of both dye concentrations in binary solutions.

Optimization of NOAC-based adsorption process for simultaneous removal of BR46 and BY13 dyes

In order to obtain the maximum removal percentages of both dyes, the effects of different parameters such as pH, adsorbent dose, sonication time, initial dye concentration and temperature on the simultaneous dye removal were studied and optimized using the batch adsorption method (Fig. 3a–d).
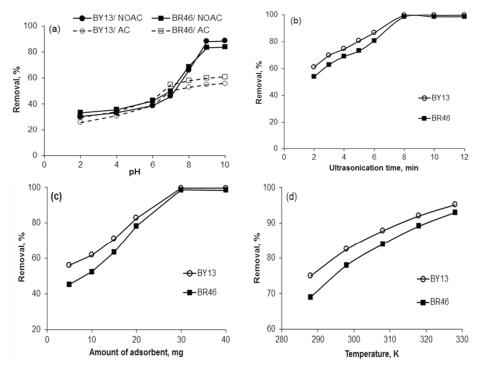

Fig. 3. Effect of different parameters on the adsorption of BY13 and BR46 dyes onto NOAC: a) solution pH for both the AC and NOAC adsorbents, b) ultrasonication time, c) adsorbent dosage and d) temperature; conditions: 100 mL of 150 mg L^{-1} dyes solution, a) t = 6 min, m = 30 mg, T = 25 ºC; b) pH 9, m = 30 mg, T = 25 ºC; c) pH 9, t = 8 min, T = 25 ºC; d) pH 9, m = 30 mg, t = 8 min.

Effect of the solution pH

The influence of the solution pH on the simultaneous removal of BY13 and BR46 dyes from binary solution by the pristine and the nitrogen modified AC samples was separately studied over the pH range of 2–10 in conditions of 150 mg L^{-1} of the binary dyes solution, 30 mg adsorbent, 6 min ultrasonication time and 25 °C, according to the general adsorption procedure. As depicted in Fig. 3a, using NOAC adsorbent (pH_{PZC} 7.9) the removal percentages of both dyes were improved with the increase of solution pH from 2 to 9 and then constant to 10. Consequently, pH 9 was chosen as optimum for all further studies.

The electrostatic interactions control the adsorption of ionic compounds significantly. For the low pH values (pH < pH_{PZC}), since the surface charge of the adsorbent is positive (because of the protonation of nitrogen and oxygen-containing groups), the electrostatic repulsion between the cationic dye molecules and the positively charged adsorbent surface decreases the adsorption of both dyes. For high pH values (pH > pH_{PZC}), the surface of the adsorbent is charged negatively (due to the deprotonation reaction) and the adsorption of dyes increases due to the electrostatic attraction between the negatively charged adsorbent surface and the cationic dye molecules.

As shown in Fig. 3a, using the pristine AC (pH_{PZC} 6.3) the similar observations were also obtained, whereas, the removal percentages of the cationic dyes were low and the quantitative removal values (< 60 %) were observed in the pH range of 7–10 (pH > pH_{PZC}). This is due to the lower density of oxygen-containing groups on AC, which deprotonated at this pH range. So, it can be concluded that physisorption is the main mechanism for dye adsorption by pristine AC.

Effect of ultrasonic-assisted adsorption time

The ultrasound irradiation is well known to accelerate a chemical process, due to the phenomenon of the acoustic cavitation. Recently an ultrasonic assisted adsorption process has been developed to favour the kinetic of the mass-transfer process of the adsorbate to the adsorbent and to reduce the time required for adsorption.[18] In this study, the different ultrasonication times from 2 to 12 min were investigated with 100 mL of 150 mg L^{-1} binary dyes solution (pH 9) containing 30 mg of NOAC at 25 °C. Fig. 3b indicates that with the increase in time, the adsorption rate of the both BR46 and BY13 dyes over the adsorbent increased and the adsorption process reaches the equilibrium in only 8 min and then remained constant up to 12 min. From the results, 8 min ultrasonication time was required to bring the complete saturation of the active sites of adsorbent, which is excellent for the synthesized NOAC; this was therefore selected as the optimum ultrasonication time for further experiments.

Effect of adsorbent amount

To optimize the adsorbent dosage for the removal of BY13 and BR46 from aqueous solutions, the adsorption experiments were performed using different adsorbent amounts (5–35 mg) at the optimum pH and contact time, according to the general procedure. As shown in Fig. 3c, the removal percentage of cationic dyes increased from 45.3 to 98.5 % for BR46 and from 56.1 to 99.6 % for BY13, with the increase of the adsorbent dose from 5 to 30 mg. This result is due to the increase in the adsorbent surface area and the availability of more adsorption sites stemming from the increased dose. However, no significant changes in the removal efficiency were observed for higher adsorbent doses (>30 mg) due to the fact that the dyes concentration on the surface of the adsorbent and in the solution came to equilibrium with each other. Accordingly, 30 mg of NOAC was used in all subsequent experiments.

Effect of temperature

The batch adsorption of BY13 and BR46 were carried out at five different temperatures in the range of 288–328 K with 100 mL of 150 mg L^{-1} binary dyes solution and 20 mg of NOAC at pH 9, and the ultrasonication time of 8 min. As can be seen in Fig. 3d, the removal efficiencies of both dyes by NOAC increase with the rise in solution temperature from 15 to 55 °C; suggesting that the adsorption process is endothermic. The kinetic energy of dyes increases with increasing temperature and this situation leads to an increased tendency of dyes to towards the adsorbent surface and consequently more adsorption onto NOAC.

Adsorption isotherms

The equilibrium isotherm plays an important role in the predictive modelling for the analysis and the design of adsorption systems. In this study, the dye removal process was analyzed using the well-known Langmuir, Freundlich and Tempkin models, according to the procedure given in "Experimental" with the various initial dye concentrations and constant values of the other parameters, for both the single and binary solutions.

The isotherm constants calculated from the linear forms of the Langmuir, Freundlich and Tempkin isotherms, along with the regression coefficient values (R^2) for three experimental conditions were listed in Table IV. The comparison of the correlation coefficients (R^2) of the linear isotherm plots indicated that for the adsorption of dyes onto NOAC in the single and binary solutions, the Langmuir isotherm yielded a much better fit than the other models at all dye concentrations (Fig. S-4 of the Supplementary material). It was observed that the equilibrium uptake amounts of BY13 and BR46 dyes in binary mixture onto NOAC decreased considerably with the increase of the concentration of the other dye, resulting in their antagonistic effect. As it can be seen from Table S-IV, the

values of R_L were in the range of 0–1, confirming the favourable uptake of both dyes onto NOAC. Therefore, the uptake of cationic dyes by NOAC in single and binary systems preferably followed the monolayer adsorption process.

TABLE IV. Isotherm parameter values for removal of BY13 and BR46 by NOAC from single and binary solutions (sample volume 100 mL, pH 9, $m = 30$ mg, $t = 8$ min, $T = 25$ °C)

System	Dye	c_0 mg L^{-1}	Langmuir			Freundlich			Temkin		
			q_{max} mg g^{-1}	K_L L mg^{-1}	R^2	K_F	n	R^2	K_T L mg^{-1}	B_T kJ mol^{-1}	R^2
Single	BY	200–400	1250	0.186	0.993	528.48	5.72	0.985	21.33	149.97	0.962
	BR	200–400	1111	0.188	0.995	519.47	6.90	0.985	26.05	138.05	0.966
Binary (1)[a]	BY	150–350	909	0.324	0.997	523.22	8.83	0.961	177.24	751.24	0.929
	BR	150–350	769	0.342	0.999	454.86	8.74	0.990	466.85	71.10	0.989
Binary (2)[b]	BY	150–350	833.3	0.265	0.993	509.28	8.63	0.978	757.48	75.98	0.967
	BR	150–350	555.6	0.414	0.999	511.68	22.03	0.431	47.1×10^7	25.31	0.403

[a]Binary system with constant concentration of the other dye :150 mg L^{-1}; [b]binary system with variable concentrations of the other dye: 150–350 mg L^{-1}

Comparison of the developed NOAC-based adsorption method with others

A comparison of the maximum adsorption capacity and the main adsorption factors of the developed NOAC-based batch adsorption method with the other published adsorption methods for the removal of BR46 and BY13 dyes from single and binary systems[2,14,22–27] were reported in Table V. Obviously, the adsorption capacity of NOAC used in this study is significantly high for single and binary systems. This may be attributed to the acid-base character of the carbon surface, its high surface area, the micropore volume and the pore size distribution. Furthermore, the type and the concentration of the active sites of adsorbents are responsible for the variation in maximum adsorption capacities between the adsorbents. As can be further seen from Table V, the considerably short contact time (8 min) along with the economic consumption of the small amount of adsorbent (30 mg) for the developed NOAC-based adsorption process is a big improvement for the dye removal from single and binary solutions. Therefore, NOAC can be considered to be an efficient and a potential adsorbent for the removal of BR46 and BY13 from single and binary solutions.

Adsorption kinetics

The characteristic constants of the adsorption kinetics were determined using the pseudo-first-order, the pseudo-second-order and the intraparticle diffusion models at various ultrasonication times (2–6 min) and the optimized values of the other parameters, according to the procedure described in "Experimental".

The calculated parameters and their corresponding R^2 values are presented in Table VI. It can be seen that the pseudo-second-order kinetic model provides a good correlation coefficients (R^2 close to 1) which suggests that the simultaneous

adsorption of BY13 and BR46 on NOAC can be better represented by the pseudo-second order model (Fig. S-5). This model is based on the assumption that the rate limiting step may be a chemical sorption involving the valence forces through sharing or exchange of electrons between the adsorbent and the adsorbate.

TABLE V. Comparison of the optimized conditions and maximum adsorption capacity of the NOAC-based adsorption method with other reported methods for removal of BR46 and BY13 from single and binary solutions

| Dye | Adsorbent | System | Optimized conditions | | | q_{max} / mg g^{-1} | | Ref. |
			Dye concentration, mg L^{-1}	Adsorbent dose, g L^{-1}	Contact time min	BY13	BR46	
BR46, BY28	Bentonite	S[a] B[b]	100–400	1.00	120	–	S: 333 B: 208	2
BB41, BR18 and BR46	Graphene oxide	S B	50	0.16	60	–	S: 476 B: 625	14
BR46	Cerbera odollam AC	S	60	0.20	120	–	456	22
BR46	Ni oxide NPs-diatomite	S	25–55	0.05	60	–	124.35	23
BR 46, BY28	Boron industry waste	S	50–300	2.00	60	–	74.73	24
BY13	Wheat bran	S	50–1000	4.00	30	69.06	–	25
BY13	Apricot stone AC	S	50–1000	6.00	35	134.59	–	26
BY13	Sepiolite	S	25–500	0.50	180	62.5	–	27
BR 46, BY13	NOAC	S	200–400	0.30	8	1111	1250	This study
		B	150–350	0.30	8	769	909	

[a]Single; [b]binary

TABLE VI. Kinetic parameter values for removal of BY13 and BR46 by NOAC from binary solutions (100 mL of 150 mg L^{-1} dyes solution, pH 9, m = 30 mg, t = 2–6 min, T = 25 °C)

| Kinetic model | Constant | Metal ion | |
		BY13	BR46
Pseudo-first order	q_1 / mg g^{-1}	335.49	348.94
	k_1 / min^{-1}	0.263	0.219
	R^2	0.981	0.978
Pseudo-second order	q_2 / mg g^{-1}	555.56	526.32
	k_2 / g mg^{-1} min^{-1}	10.41×10^{-4}	9.49×10^{-4}
	R^2	0.9935	0.9909
Intra-particle diffusion	C_i	305.40	270.32
	k_i / mg min$^{-1/2}$ g^{-1}	3.755	3.874
	R^2	0.9561	0.9480

Adsorption thermodynamics

The thermodynamic behaviour of the simultaneous adsorption of BY13 and BR46 on NOAC were further investigated in the temperature ranges of 288–328 K, according to the procedure given in the "Experimental". The thermodynamic parameters such as Gibbs energy (ΔG), enthalpy (ΔH) and entropy change (ΔS^0) were calculated.[21]

The thermodynamic parameters are presented in Table VII. For the adsorption of both dyes onto NOAC, the obtained ΔH values were positive which indicates the endothermic nature of the adsorption process, which is in good agreement with the results that show that the adsorption of dyes increased with the temperature. The negative ΔG values showed the spontaneous nature of the adsorption process. Also, the positive values of ΔS show the increased randomness at the solid/solution interface.

TABLE VII. Thermodynamic parameters for removal of BY13 and BR46 by NOAC from binary solutions (100 mL of 150 mg L^{-1} dyes solution, pH=9, m=30 mg, t= 8 min)

Dye	Parameter	T / K				
		288	298	308	318	328
BY13	ΔH / kJ mol^{-1}	36.51	36.51	36.51	36.51	36.51
	ΔG / kJ mol^{-1}	–5.513	–6.825	–8.125	–9.640	–11.418
	ΔS / kJ mol^{-1} K^{-1}	0.146	0.146	0.146	0.146	0.146
BR46	ΔH / kJ mol^{-1}	34.57	34.57	34.57	34.57	34.57
	ΔG / kJ mol^{-1}	–2.499	–5.133	–8.329	–12.365	–17.334
	ΔS / kJ mol^{-1} K^{-1}	0.136	0.136	0.136	0.136	0.136

Desorption and regeneration studies

An ideal adsorbent should exhibit not only the high sorption capacity, but also the easy regeneration and stability during several adsorption–desorption cycling, which can significantly reduce the overall cost of the adsorbent. Desorption studies also help to elucidate the nature of adsorption and the recycling of the spent adsorbent and the dye.[20] First, the best desorption solvent was selected according to the procedure explained in the "Experimental" and then the number of the adsorption-desorption cycles using this solvent were investigated.

Fig. S-6a and b show the effects of various solvents for desorption of BY13 and BR46 dyes from NOAC, respectively. Among these, HCl (2.0–3.0 mol L^{-1}) and H$_2$SO$_4$ (3.0 mol L^{-1}) solutions provided higher desorption efficiency ($R \approx 100$ %) for both BY13 and BR46. Thus, in order to use low concentration of an organic solvent, HCl (2.0 mol L^{-1}) was specified as the best solvent for the quantitative desorption of dyes. This indicates that the adsorption of dyes onto NOAC is performed through ion exchange. In an acidic medium due to the protonation, the electrostatic interactions between the adsorbent surface and the cationic dyes become weaker, and then the adsorbed dyes leave the adsorption site.

In order to investigate the long-term stability of NOAC, it was subjected to several adsorptions and desorption cycles under the optimized conditions, as described above. The adsorption process was started with fresh NOAC and after the desorption step, using 100 mL of HCl (2.0 mol L^{-1}), the regenerated adsorbent was reused for the subsequent adsorption-desorption cycle. As shown in Fig. 4, the NOAC nanosorbent can be used for 5 adsorption–desorption cycles without the decrease in the removal percentages of BY13 and BR46. At the sixth cycle, the removal percentages of BY13 and BR46 were decreased to 96 and 94 %, respectively. However, after 16 adsorption-desorption cycles, the removal percentages of BY13 and BR46 were decreased to 16% and 45%, respectively.
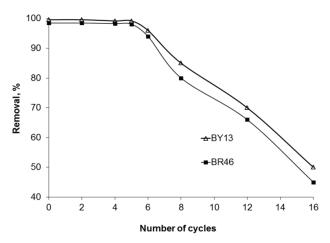

Fig. 4. Reusability of the NOAC under the optimized conditions.

CONCLUSIONS

In the present paper, the eucalyptus leaves-based nanoporous activated carbon was prepared *via* the chemical activation with KOH, oxidized with nitric acid, then modified with urea, and finally introduced as a new and efficient adsorbent for simultaneous ultrasound assisted removal of BR46 and BY13 dyes from binary solutions. The AC and NOAC both generated the high specific surface area and the high micro pore volume. The first-order derivative spectrophotometric method was successfully applied for the determination of BY13 in binary solutions. The optimum conditions of batch adsorption were found to be pH 9, initial BR and BY concentrations of 150 mg L^{-1}, NOAC dosage of 30 mg, sonication time of 8 min, and temperature 25 °C. The data indicated that the adsorption kinetics of dyes on NOAC followed the pseudo-second order. The equilibrium data were correlated considerably well by the Langmuir adsorption isotherm in both the single and binary mixtures. Based on the thermodynamic studies, the adsorption of dyes was both endothermic and spontaneous. The rem-

arkable advantages of the developed NOAC-based adsorption process include its high removal performance (>98.5 %) for a very short time and the economic consumption of only 30 mg of NOAC adsorbent which has superior adsorption capacities and can also be regenerated and reused for 5 adsorption-desorption cycles. In conclusion, NOAC can be effectively used as an adsorbent for the removal of cationic dyes from single and binary systems.

SUPPLEMENTARY MATERIAL

Aditional data and information are available electronically at the pages of journal website: http://www.shd.org.rs/JSCS/, or from the corresponding author on request.

ИЗВОД

НИТРОГЕНИЗОВАНИ АКТИВНИ УГАЉ ОД ЕУКАЛИПТУСОВОГ ЛИШЋА СА НАНОПОРАМА ЗА УЛТРАЗВУЧНО УКЛАЊАЊЕ ОСНОВНИХ БОЈА УЗ КОРИШЋЕЊЕ ДЕРИВАТИВНЕ СПЕКТРОСКОПИЈЕ

AISAN KHALIGH[1], HASSAN ZAVVAR MOUSAVI[1], ALIMORAD RASHIDI[2] и HAMID SHIRKHANLOO[3]

[1]Department of Chemistry, Semnan University, Semnan 35131-1911, Iran, [2]Nanotechnology Research Center, Research Institute of Petroleum Industry (RIPI), West Entrance Blvd., Olympic Village, Tehran 14857-33111, Iran и [3]Research Institute of Petroleum Industry (RIPI), West Entrance Blvd., Olympic Village, Tehran 14857-33111, Iran

Активни угаљ од еукалиптусовог лишћа са нанопорама (AC) је припремљен од еукалиптусовог лишћа хемијском активацијом помоћу KOH, а затим третиран азотном киселином/уреом (NOAC) и коначно употребљен као нови адсорбенс за истовремено ултразвучно уклањање основне црвене 46 (BR46) и основне жуте 13 (BY13) боје из бинарних водених раствора. Наноадсорбенс NOAC је окарактерисан SEM, TEM, Раман, BET, FTIR, CXN, pH_{pzc} и Boehm титрационим анализама. И AC и NOAC узорци су имали суприорну BET површину од 2222 и 1572 m^2 g^{-1} са просечном запремином микропора од 0,81 и 0,50 cm^3 g^{-1}, редом. За анлизу BY13 бинарних смеша коришћена је деривативна спектроскопија првог реда. Мала количина адсорбента (30 mg) је била способна да уклони висок проценат боја (>99 %) за врло кратко време (8 min). Адсорпција боја је пратила Лангмирову изотерму и кинетику псеудопрвог реда. Адсорпциони капацитети NOAC за просте растворе BR46 и BY13 били су 1111 и 1250 mg g^{-1}, а за бинарне растворе 769 и 909 mg g^{-1}, редом. Испитана је и адсорпциона термодинамика. Истрошени NOAC је регенерисан коришћењем HCl (2 M) и поново употребљен за пет циклуса адсорпција––десорпција уз веома успешне перформансе.

(Примљено 27. августа, ревидирано 17. октобра, прихваћено 25. октобра 2017)

REFERENCES

1. S. Nethaji, A. Sivasamy, A. Mandal, *Int. J. Environ. Sci. Technol.* **10** (2013) 231
2. M. Turabik, *J. Hazard. Mater.* **158** (2008) 52
3. K. Singh, S. Arora, *Crit. Rev. Env. Sci. Tec.* **41** (2011) 807
4. Z. Y. Velkova, G. K. Kirova, M. Stoytcheva, V. Gochev, *J. Serb. Chem. Soc.* **82** (2017) 1
5. M. A. Yahya, Z. Al-Qodah, C. Z. Ngah, *Renew. Sustainable Energy Rev.* **46** (2015) 218

6. A. M. Rashidi, D. Kazemi, N. Izadi, M. Pourkhalil, A. Jorsaraei, E. Ganji, R. Lotfi, *Korean J. Chem. Eng.* **33** (2016) 616
7. J. Rivera-Utrilla, M. Sánchez-Polo, V. Gómez-Serrano, P. Alvarez, M. Alvim-Ferraz, J. Dias, *J. Hazard. Mater.* **187** (2011) 1
8. M. H. Kasnejad, A. Esfandiari, T. Kaghazchi, N. Asasian, *J. Taiwan Inst. Chem. Eng.* **43** (2012) 736
9. T. X. Shang, J. Zhang, X. J. Jin, J. M. Gao, *J. Wood Sci.* **60** (2014) 215
10. S. Bashkova, T.J. Bandosz, *J. Colloid Interface Sci.* **333** (2009) 97
11. L. Monser, N. Adhoum, *Sep. Purif. Technol.* **26** (2002) 137
12. J. Zhu, B. Deng, J. Yang, D. Gang, *Carbon* **47** (2009) 2014
13. E. Lorenc-Grabowska, G. Gryglewicz, M. Diez, *Fuel* **114** (2013) 235.
14. Z. Hosseinabadi-Farahani, H. Hosseini-Monfared, N.M. Mahmoodi, *Desal. Water Treat.* **56** (2015) 2382
15. M. Tarighat, *Int. J. Environ. Sci. Technol.* **13** (2016) 11
16. D. Hulicova Jurcakova, M. Seredych, G.Q. Lu, T.J. Bandosz, *Adv. Funct. Mater.* **19** (2009) 438
17. S. M. Lee, D. Tiwari, *Chem. Eng. J.* **225** (2013) 128
18. M. Roosta, M. Ghaedi, A. Daneshfar, R. Sahraei, A. Asghari, *Ultrasonics Sonochem.* **21** (2014) 242
19. F. Li, Y. Chen, H. Huang, W. Cao, T. Li, *Chem. Eng. Res. Des.* **100** (2015) 192
20. M. Hema, S. Arivoli, *J. Appl. Sci. Environ. Manag.* **12** (2008)
21. M.A. Ahmad, N.A.A. Puad, O.S. Bello, *Water Resour. Ind.* **6** (2014) 18
22. N. Azmi, N. Zainudin, U. Ali, F. Senusi, *J. Eng. Sci. Technol.* **5** (2015) 82
23. M. Yazdanshenas, K. Farizadeh, A. Fazilat, S. Ahmadi, *J. Appl. Chem. Res.* **8** (2014) 15
24. A. Olgun, N. Atar, *J. Hazard. Mater.* **161** (2009) 148
25. M. Sulak, E. Demirbas, M. Kobya, *Bioresour. Technol.* **98** (2007) 2590
26. E. Demirbas, M. Kobya, M. Sulak, *Bioresour. Technol.* **99** (2008) 5368
27. M. Tekbaş, N. Bektaş, H.C. Yatmaz, *Desalination* **249** (2009) 205.